Journal of Solid State Chemistry 181 (2008) 3110–3115

Contents lists available at ScienceDirect

Journal of Solid State Chemistry

journal homepage: www.elsevier.com/locate/jssc

A new lithium manganese phosphate with an original tunnel structure in the $A_2MP_2O_7$ family

Laure Adam, Anne Guesdon *, Bernard Raveau

[a] Laboratoire CRISMAT, UMR 6508 CNRS ENSICAEN, Université de Caen Basse-Normandie, 6 Boulevard du Maréchal Juin, 14050 CAEN Cedex, France

ARTICLE INFO

Article history:
Received 12 June 2008
Received in revised form
24 July 2008
Accepted 26 July 2008
Available online 14 August 2008

Keywords:
Solid-state synthesis
Single-crystal XRD
Intersecting tunnels structure
Mixed framework
Lithium manganese diphosphate

ABSTRACT

A new member of the $A_2MP_2O_7$ diphosphate family, $Li_2MnP_2O_7$, has been synthesized by solid-state reaction and characterized using single-crystal X-ray diffraction. $Li_2MnP_2O_7$ crystallizes in the monoclinic space group $P2_1/a$ (#14) with the cell parameters $a = 9.9158(6)$ Å, $b = 9.8289(6)$ Å, $c = 11.1800(7)$ Å, $\beta = 102.466(5)^\circ$, $Z = 8$ and $V = 1063.9(1)$ Å^3. Its mixed framework exhibits an original Mn_2O_9 unit, built up of one MnO_5 trigonal bipyramid sharing one edge with one MnO_6 octahedron. These Mn_2O_9 units are sharing corners with P_2O_7 diphosphate groups, forming the undulating $[Mn_4P_8O_{32}]_\infty$ layers. The $[MnP_2O_7]_\infty$ 3D framework, resulting from the interconnection of the undulating $[Mn_4P_8O_{32}]_\infty$ layers, exhibits different kinds of intersecting tunnels containing the Li cations.

1. Introduction

The search for new cathode materials for rechargeable lithium batteries makes that mixed frameworks built up of transition metal polyhedra and PO_4 tetrahedra are of great interest, as shown from the discovery of the performances of the famous olivine phosphate $LiFePO_4$ [1–3]. Besides iron, other elements such as manganese, nickel or cobalt have been investigated in view of understanding the influence of the structure on the electrochemical performances of these $LiMPO_4$ oxides as cathodic materials [4,5].

Thus, it appears that the lithium transition metal phosphates can be considered as having a potential for the generation of new cathode materials. In this respect, the lithium manganese phosphates are very interesting, due to the fact that manganese can exhibit several oxidation states, Mn(II), Mn(III) and Mn(IV). In fact, a very limited number of lithium manganese phosphates have been synthesized to date. Besides the two forms of $LiMnPO_4$ [6] only two other anhydrous manganese phosphates are actually known: the Mn(II) phosphate $LiMn(PO_3)_3$ [7] and the Mn(III) diphosphate $LiMnP_2O_7$ [8]. The chemistry of the lithium manganese phosphate hydrates and hydroxyphosphates is still more restricted, since only two compounds have been synthesized to date to our knowledge, the Mn(II) cyclohexaphosphate decahydrate $Li_2MnP_6O_{18} \cdot 10H_2O$ [9] and the Mn(III) hydroxide monophosphate $LiMn(OH)PO_4$ [10]. We have thus revisited the system Li–Mn–P–O and we report herein on a new diphosphate $Li_2MnP_2O_7$, with an original tunnel structure. The $[MnP_2O_7]_\infty$ framework is unique, compared to all the other $A_2MP_2O_7$ phosphates, due to the presence of Mn_2O_9 units built up of one MnO_6 octahedron and one MnO_5 polyhedron sharing one edge and interconnected through P_2O_7 groups.

2. Experimental

2.1. Synthesis

The single crystal used for the structure determination of $Li_2MnP_2O_7$ was extracted from a preparation of nominal composition $Li_2MnP_2O_7$ synthesized in two steps. First Li_2CO_3 (Prolabo, 99.9%), Mn_2O_3 (Alfa Aesar, 98%) and $(NH_4)_2HPO_4$ (Prolabo Normapur, 99.5%) were mixed in an agate mortar. The mixture was placed in a platinum crucible and heated in air at about 600 °C for a few hours until the correct weight loss was reached, i.e. when Li_2CO_3 and $(NH_4)_2HPO_4$ had decomposed. In a second step, metallic Mn (Acros Organics, 99%) was added to the resulting powder and the new mixture was finely ground in an agate mortar and then placed in a silica tube, which was evacuated and sealed. The silica tube was heated at 800 °C for 15 h before being slowly cooled at a rate of 2 °C h^{-1} to 700 °C and then brought back to room temperature. A grey solid-like powder containing a mixture of $LiMnPO_4$ [6], $Li_2Mn(PO_3)_4$ [11] and colourless crystals of the title compound was thus obtained.

* Corresponding author. Fax: +33 2 31 95 16 00.
E-mail address: anne.guesdon@ensicaen.fr (A. Guesdon).

0022-4596/$ - see front matter © 2008 Elsevier Inc. All rights reserved.
doi:10.1016/j.jssc.2008.07.039

A single-phased sample has been synthesized in a similar way as described above, i.e. in two steps, starting from a mixture of MnO (Alpha Aesar, 99.99%), Li_2CO_3 and $(NH_4)_2HPO_4$. The mixture was first heated in air at about 600 °C for a few hours, and then placed in an evacuated silica tube which was heated at 650 °C for 15 h, cooled to 550 °C at a rate of 2 °C h^{-1}, and then brought back to room temperature. The sample was confirmed to be monophasic by using X-ray powder diffraction. All diffraction peaks could indeed be indexed in a monoclinic cell ($P2_1/a$ space group) with the following cell parameters: $a = 9.8945(1)$ Å, $b = 9.8113(1)$ Å, $c = 11.1596(1)$ Å, $\beta = 102.485(1)^\circ$ (refinement performed using the program JANA 2006 [12] in the pattern matching mode).

2.2. Crystal studies: EDX analysis and X-ray diffraction

Semi-quantitative analyses of some colourless crystals extracted from the preparation were performed with an EDAX microprobe mounted on a ZEISS Supra 55 scanning electron microscope. They revealed the presence of Mn and P elements in the approximative ratio 1–2 in the crystals, in agreement with the composition deduced from the single-crystal X-ray diffraction study. Several crystals were then optically selected to be tested. A single crystal, with dimensions $0.103 \times 0.052 \times 0.026$ mm^3, was chosen for the structure determination and refinement. The data were collected with a Bruker–Nonius Kappa CCD four-circle diffractometer equipped with a bidimensional CCD detector and using the Mo-$K\alpha$ radiation. Strategy using φ and ω scans with 0.5° frame^{-1}, 100 s/°, two iterations, was determined. The crystal–detector distance was fixed at $D_x = 34$ mm. Data were reduced and corrected for Lorentz and polarization effects with the EvalCCD [13] package. The observed reflection conditions $h\,0\,l$: $h = 2n$, $0\,k\,0$: $k = 2n$, $h\,0\,0$: $h = 2n$ were compatible with the $P2_1/a$ space group (#14). The data were corrected from absorption effects using SADABS (Bruker–Nonius area detector scaling and absorption correction version 2.10). The structure was solved and refined in this centrosymmetric space group, using the JANA2006 program [12]. The structure of $Li_2MnP_2O_7$ was determined using the heavy atom method and successive difference synthesis and Fourier synthesis. First Mn, P and O atoms were located. The refinement of their atomic coordinates and anisotropic thermal parameters led to the reliability factors $R = 0.0733$ and $R_w = 0.1048$. The maximum of residual electronic densities observed on Fourier difference was 8.31 e Å^{-3}. At this step of the refinement, four independent lithium atoms could be located using the distances between Fourier maxima and oxygen atoms. Li atomic coordinates and anisotropic thermal parameters were refined and secondary extinction effect corrections were applied, leading to the reliability factors $R = 0.0363$ and $R_w = 0.0387$. The maximum of residual electronic densities was 0.62 e Å^{-3}. Table 1 gives the data collection, cell and refinement parameters for single-crystal X-ray diffraction study. The resulting atomic parameters are listed in Table 2. Bond valence sum (BVS) calculations [14] performed for lithium, manganese and phosphorus cations and oxygen anions lead to the expected values of 1, 2, 5 and 2, respectively. Tables of the anisotropic displacement parameters for all atoms and detail of the bond valence calculations are available as Supplementary material.

Further details of the crystal structure investigation can be obtained from the Fachinformationszentrum Karlsruha, 76344 Eggenstein-Leopoldshafen, Germany (fax: +49 7247 808 666; e-mail: crysdata@fiz.karlsruhe.de) on quoting the deposit number CSD 419562.

Table 1
Data collection cell and refinement parameters for single-crystal X-ray diffraction study

Crystal data	
Chemical formula	$Li_2MnP_2O_7$
M (g mol^{-1})	242.76
Cell setting, space group	Monoclinic, $P2_1/a$
Atomic parameters	$a = 9.9158$ (6) Å
	$b = 9.8289$ (6) Å
	$c = 11.1800$ (7) Å
	$\beta = 102.466$ (5)°
V (Å^3)	1063.9 (1)
Z	8
ρ_{calc} (g cm^{-3})	3.0301
Crystal size (mm^3)	$0.103 \times 0.052 \times 0.026$
Data collection	
λ (Mo$K\alpha$)	0.71069 Å
Scan strategy	φ and ω scans; 0.5° frame^{-1}; 100 s/°; two iterations
	$D_x = 34$ mm
θ range and limiting indices	$5.76° \leqslant \theta \leqslant 40°$; $0 \leqslant h \leqslant 17$, $0 \leqslant k \leqslant 17, -20 \leqslant l \leqslant 20$
Measured reflections	20499
Independent reflections	6021
μ (mm^{-1})	3.062
Structure solution and refinement	
Parameters refined	217
Agreement factors	$R = 3.63\%$; $R_w = 3.87\%$
Weighting scheme	$w = 1/\sigma(F)^2$

Table 2
Refined atomic parameters and their estimated standard deviations for $Li_2MnP_2O_7$

Atoms	x	y	z	U_{eq}[a] (Å^2)
Mn1	0.24502(3)	0.71349(3)	0.17850(3)	0.01010(8)
Mn2	0.29847(3)	0.41987(3)	0.32451(3)	0.00971(8)
P1	0.37664(5)	0.65002(5)	0.57237(5)	0.00680(11)
P2	0.05902(5)	0.93196(5)	0.24432(5)	0.00726(12)
P3	0.02599(5)	0.45499(5)	0.76037(5)	0.00712(11)
P4	0.61877(5)	0.79625(5)	−0.10854(5)	0.00746(12)
O1	0.16246(14)	0.82821(14)	0.31350(14)	0.0114(4)
O2	0.48113(14)	0.77732(15)	−0.07557(14)	0.0129(4)
O3	0.38378(14)	0.86486(14)	0.14432(13)	0.0121(4)
O4	0.02156(13)	0.84084(14)	0.55022(13)	0.0108(4)
O5	0.43627(15)	0.43440(15)	−0.11127(13)	0.0129(4)
O6	0.18198(14)	0.83005(14)	−0.15145(13)	0.0110(4)
O7	0.02235(15)	0.41597(15)	0.62905(13)	0.0128(4)
O8	0.18629(15)	0.28940(14)	0.41843(13)	0.0114(4)
O9	0.09527(14)	0.60349(14)	0.77455(13)	0.0094(3)
O10	0.38830(14)	0.58020(14)	0.70422(13)	0.0093(3)
O11	0.41492(13)	0.58835(14)	0.26962(13)	0.0103(4)
O12	0.27481(14)	0.56376(14)	0.48188(13)	0.0116(4)
O13	0.37991(13)	1.03269(14)	−0.21286(13)	0.0096(3)
O14	0.22241(14)	0.63316(15)	−0.00380(13)	0.0112(4)
Li1	0.6548(3)	0.0866(4)	0.0422(3)	0.0114(9)
Li2	0.0855(4)	0.1081(4)	0.0288(4)	0.0141(10)
Li3	0.6654(6)	0.0748(5)	0.5423(5)	0.0397(19)
Li4	0.3898(4)	0.2223(4)	0.5523(4)	0.0161(11)

[a] The atomic displacement parameters of all atoms were refined anisotropically and are given in the form of an equivalent isotropic displacement parameter defined by $U_{eq} = \frac{1}{3}\sum_{i=1}^{3}\sum_{j=1}^{3} U_{ij} a^{*i} a^{*j} \vec{a}_i \vec{a}_j$.

2.3. Magnetic characterization

Magnetic susceptibility data were collected on a 65.86 mg powder sample of $Li_2MnP_2O_7$, from 5 to 400 K in a 0.3 T field, using a Quantum Design SQUID magnetometer.

3. Results and discussion

In this new structure, the manganese polyhedra and phosphate tetrahedra form a 3D $[MnP_2O_7]_\infty$ framework built up of MnO_5

trigonal bipyramids (Mn1), MnO_6 octahedra (Mn2) and diphosphate groups P_2O_7 (P1–P2 and P3–P4) (Fig. 1). The great originality of this manganese diphosphate deals with the fact that one MnO_5 bipyramid and one MnO_6 octahedron share one edge (O11–O13) to form Mn_2O_9 units (Figs. 1a and 2), interconnected through P_2O_7 groups. It results in the formation of two sorts of tunnels running along **a** (Fig. 1a) and a third sort of tunnels running along **b** (Fig. 1b). The lithium cations are sitting in these different tunnels.

In fact, the entire $[MnP_2O_7]_\infty$ framework can be described by the stacking along **c** of identical $[Mn_4P_8O_{32}]_\infty$ undulating layers parallel to (0 0 1) (Fig. 1). In each layer (Fig. 2), one Mn_2O_9 unit alternates with two P_2O_7 units along **b** forming undulating $[Mn_2P_4O_{19}]_\infty$ chains running along that direction. In such chains (Fig. 2b), each Mn1 bipyramid is linked to two diphosphate groups: it shares one apex (O3) with the P3 tetrahedron of a "P3–P4" group and one apex (O1) with the P2 tetrahedron of a "P1–P2" diphosphate group. The P1 and P4 tetrahedra of these two diphosphate groups are linked to the Mn2 octahedron of the next Mn_2O_9 unit of the $[Mn_2P_4O_{19}]_\infty$ chain through two apices (O8 and O6, respectively). Along **a**, two successive chains are deduced one from the other by a 2_1 axis and are connected through the corners of their polyhedra, the diphosphate groups of one chain being linked to the Mn_2O_9 units of the next chain (Fig. 2a). More precisely, the P1–P2 diphosphate groups of one chain share two apices (O4 for P1 and O11 for P2) with one Mn_2O_9 unit, P1 being connected to the Mn2 octahedron through O4 and P2 being linked both to Mn1 bipyramid and Mn2 octahedron through their common oxygen atom O11. The P3–P4 diphosphate groups are only sharing one apex with the Mn_2O_9 units, P3 being connected to the O13 oxygen atom common to the Mn1 bipyramid and Mn2 octahedron. The $[Mn_4P_8O_{32}]_\infty$ undulating layer resulting from this assembly of $[Mn_2P_4O_{19}]_\infty$ chains presents six-sided windows (Fig. 2).

Finally, each $[Mn_4P_8O_{32}]_\infty$ layer shares the apices of its Mn polyhedra in two different ways with the next layers along **c**, to form the 3D $[MnP_2O_7]_\infty$ framework (Fig. 1). On the one side, this layer shares one apex (O12) of its P1–P2 group with the Mn2 octahedron of the next layer, forming rows of five-sided [1 0 0] tunnels undulating along **b**. On the other side, it shares one apex (O14) of its P3–P4 group with the Mn1 trigonal bipyramid of the next layer, forming rows of six-sided [1 0 0] tunnels running along **b**, and rows of [0 1 0] Z-like tunnels running along **a**.

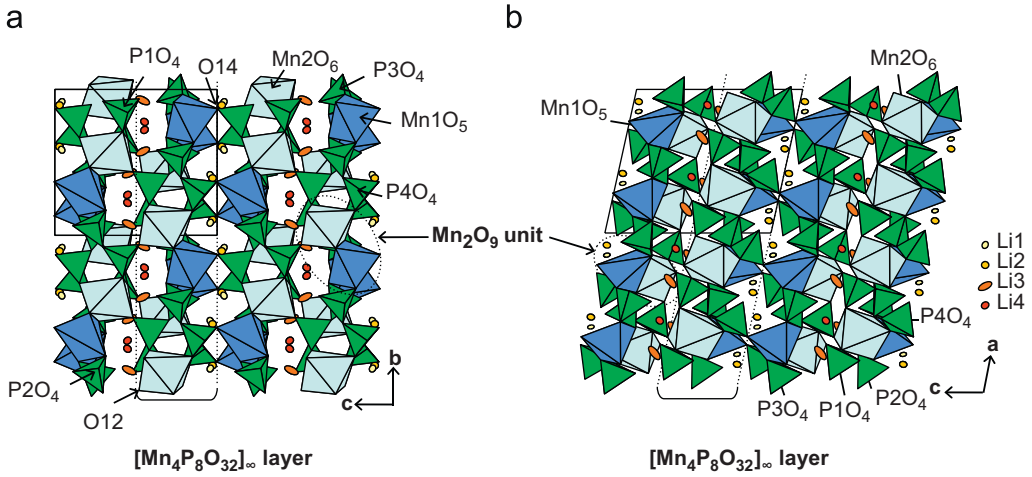

Fig. 1. Projections of the 3D structure of $Li_2MnP_2O_7$ along [100] (a) and along [010] (b), evidencing the stacking of the $[Mn_4P_8O_{32}]$ undulating planes along [0 0 1] and showing the different types of tunnels containing the lithium cations.

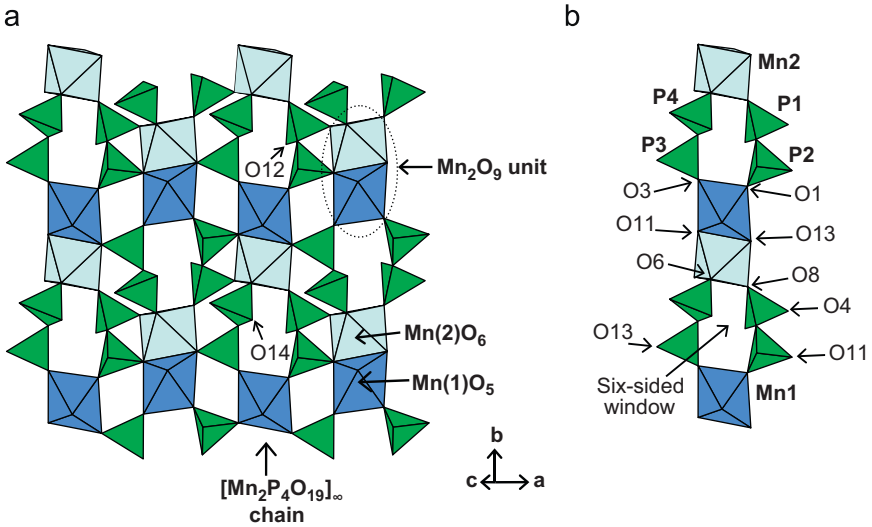

Fig. 2. (a) Projection of one $[Mn_4P_8O_{32}]_\infty$ layer on the (0 0 1) plane. The polyhedra of one $[Mn_2P_4O_{18}]_\infty$ chain have been underlined. (b) View of one $[Mn_2P_4O_{18}]_\infty$ chain, showing the connections between the different polyhedra and the six-sided windows.

The lithium cations are displayed in undulating layers parallel to (0 0 1) (Fig. 1) with various coordinations (Fig. 3). Li1 and Li2, which sit in the six-sided tunnels, exhibit a distorted square pyramidal and an almost regular tetrahedral coordination, respectively. The Li–O distances (Table 3) are comprised between 1.98 and 2.35 Å in the Li1 pyramids, and between 1.90 and 2.00 Å in the Li2 tetrahedra. Note that the Li1 and Li2 polyhedra share their edges and corners, forming $[Li_2O_6]_\infty$ layers parallel to (001). More precisely, each Li2 is linked to two different Li1 through its O14 and O2 corners and shares its O5–O5 edge with an other Li2.

Li3 and Li4, which sit in the five-sided tunnels, exhibit a distorted tetrahedral and a pseudo-square pyramidal coordination, respectively. The Li3 tetrahedra are indeed very distorted with Li–O distances ranging from 1.89 to 2.29 Å, whereas in the Li4 pyramids one observes Li–O distances ranging from 1.96 to 2.33 Å (Table 3). The Li3 and Li4 polyhedra share corners and edges, forming $[Li_2O_5]_\infty$ layers parallel to (001). In these layers, each Li4 pyramid is linked through O7 and O12 to two different Li3 tetrahedra and shares its O1–O8 edge with a third Li3 tetrahedron.

The P–O bond distances observed in the PO_4 tetrahedra are ranging from 1.50 to 1.61 Å (Table 3). As expected, each PO_4 tetrahedron presents a larger P–O bond corresponding to the P–O–P bond of the P_2O_7 diphosphate group. We can note here that P2, P3 and P4 tetrahedra exhibit one free apex, whereas P1 shares all its corners (one with P2 to form a diphosphate group and the three others with Mn polyhedra).

The MnO_5 bipyramids are quite distorted, as shown from the examination of the O–Mn1–O angles. The Mn1–O distances are comprised between 2.12 and 2.25 Å. The Mn2 octahedra exhibit a more regular geometry with Mn2–O distances ranging from 2.12 to 2.31 Å (Table 3). The magnetic susceptibility χ versus temperature and the corresponding χ^{-1} versus T for $Li_2MnP_2O_7$ are presented in Fig. 4. $Li_2MnP_2O_7$ exhibits a paramagnetic behaviour. The susceptibility follows a Curie–Weiss law with $C = 4.43\,\text{emu K mol}^{-1}$ and $\theta = -13.9(1)\,K$. The effective magnetic moment μ_{eff} calculated from the Curie constant is equal to 5.95 μ_B, this value being very close to the spin value of 5.92 μ_B expected for a high-spin Mn^{2+} (d^5) ion. These results are thus in agreement with the bond valence calculation, since they confirm the divalent state of manganese in this compound.

$Li_2MnP_2O_7$, with its original structure, represents a new member of the large family of $A_2MP_2O_7$ diphosphates. In this series, $Li_2MnP_2O_7$ is the only framework involving Mn_2O_9 units built up of one MnO_6 octahedron and one MnO_5 trigonal bipyramid sharing one edge. The various frameworks encountered in this large family of diphosphates consist indeed of isolated MO_6 octahedra interconnected through diphosphates groups, as observed for A = Na, K, Rb, Cs, Ag and M = Ca, Mn, Cd, Sr [15–19] or of isolated MO_4 polyhedra interconnected through P_2O_7 groups, as shown for A = Ag, Na, K, Li and M = Co, Cu, Pd, Zn [20–30]. Dimeric M_2O_{10} units (built up of two edge-sharing MO_6 octahedra) interconnected through P_2O_7 groups are observed only in some $A_2MP_2O_7$ phosphates for A = Na, K and M = Mn, Ni [31,32], whereas dimeric Mn_2O_{11} units (built up of corner-sharing MO_6 octahedra) seem to be still more rare, since the only example is to our knowledge $Na_2CoP_2O_7$ [20].

From a more general point of view, these Mn_2O_9 units are rarely observed in manganese(II) phosphates. To our knowledge, Mn_2O_9 units have only been observed in quite condensed phases which do not contain any template or counter-cation. They can indeed be encountered in $Mn_6(PO_4)_4(H_2O)$ [33], $Mn_7(HPO_4)_2(PO_4)_2$ [34] and $(Fe_{4.94}Mn_{2.06})(PO_4)_6$ [35]. One can however notice that, in these compounds, the Mn_2O_9 units are linked via two edges of their MnO_5 polyhedron to two Mn_2O_{10} dioctahedral units. The Mn_2O_9 unit has also been reported as the unique manganese structural unit of the structure in $Mn_3(PO_4)_2$ [36], but not as an isolated dimer since these Mn_2O_9 units share corners to form the 3D framework. The presence of Mn_2O_9 mixed units has thus never been observed in manganese(II) phosphates up to now, moreover, it is observed for the first time in a Mn(II) phosphate involving a counter-cation. The small size of the Li^+ cation may explain the existence of the Mn_2O_9 unit in $Li_2MnP_2O_7$.

Li cations environment also contributes to make $Li_2MnP_2O_7$ an original framework. As a matter of fact, in lithium manganese phosphates, the more currently observed coordination for lithium is the octahedral one. Only a few compounds present a different Li coordination: $Li_2Mn_2(P_6O_{18})(H_2O)_{10}$ [9] exhibits LiO_4 polyhedra,

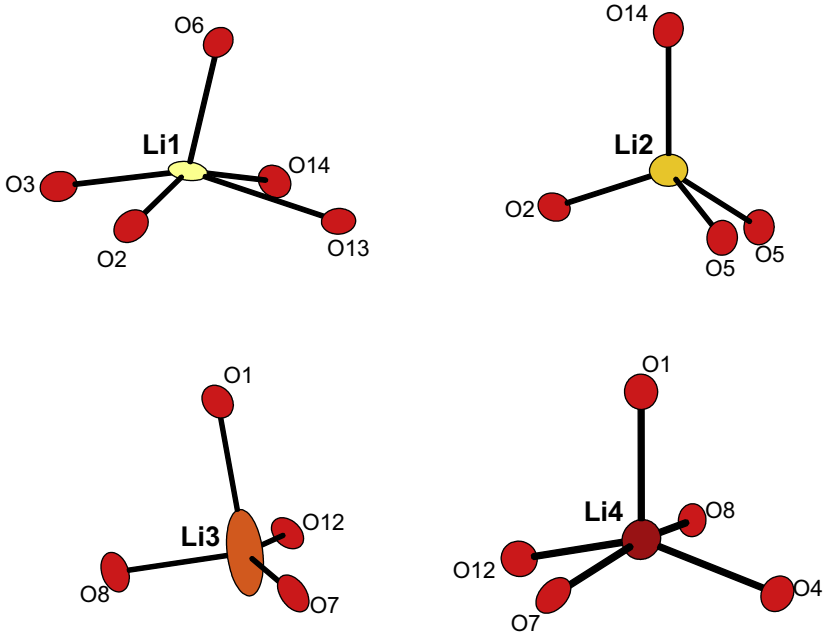

Fig. 3. Environment of the lithium cations in $Li_2MnP_2O_7$. Displacement ellipsoids are drawn at a 80% probability level.

Table 3
Selected bond distances (Å) and angles (°) in the coordination polyhedra of $Li_2MnP_2O_7$

Mn1	O1	O3	O11	O13	O14
O1	**2.1802(16)**	3.212(2)	2.5334(19)	3.110 (2)	4.186(2)
O3	96.73(6)	**2.1165(15)**	3.043(2)	2.5133(18)	3.0570(19)
O11	109.87(6)	90.81(5)	**2.1559(13)**	2.9065(18)	3.2654(18)
O13	89.28(6)	172.31(5)	82.61(5)	**2.2462(14)**	2.989(2)
O14	150.18(5)	91.48(6)	98.58(6)	85.60(6)	**2.1518(15)**

Mn2	O4	O6	O8	O11	O12	O13
O4	**2.1611(13)**	3.3727(19)	2.8866(19)	3.134 (2)	3.053(2)	4.3743(18)
O6	102.19(5)	**2.1730(15)**	3.530(2)	2.9267(19)	4.449(2)	2.979(2)
O8	84.82(5)	110.65(6)	**2.1187(16)**	4.311(2)	2.8770(19)	3.283 (2)
O11	92.40(5)	84.46(6)	164.88(6)	**2.1813(15)**	3.007(2)	2.9065(18)
O12	86.09(5)	166.11(5)	80.94(6)	84.05(6)	**2.3086(15)**	3.0823(19)
O13	170.64(5)	85.18(5)	98.09(5)	82.47(5)	85.58(5)	**2.2278(13)**

P1	O4	O8	O10	O12
O4	**1.5126(15)**	2.514(2)	2.509(2)	2.5773(19)
O8	112.11(8)	**1.5180(15)**	2.4934(19)	2.475(2)
O10	107.02(8)	105.81(8)	**1.6073(15)**	2.5027(19)
O12	116.19(9)	108.90(8)	106.12(8)	**1.5234(14)**

P2	O1	O5	O10	O11
O1	**1.5322(14)**	2.491(2)	2.5267(19)	2.5334(19)
O5	110.53(9)	**1.4985(16)**	2.472(2)	2.547(2)
O10	106.94(7)	105.23(8)	**1.6116(14)**	2.5280(19)
O11	111.74(8)	114.61(8)	107.22(8)	**1.5283(15)**

P3	O3	O7	O9	O13
O3	**1.5195(14)**	2.5526(19)	2.5072(19)	2.5127(18)
O7	114.87(9)	**1.5103(16)**	2.4609(19)	2.539(2)
O9	106.62(7)	104.28(8)	**1.6064(14)**	2.5500(19)
O13	110.15(8)	112.41(8)	107.96(8)	**1.5458(15)**

P4	O2	O6	O9	O14
O2	**1.5002(16)**	2.553(2)	2.507(2)	2.5133(18)
O6	115.90(8)	**1.5146(15)**	2.461(2)	2.540(2)
O9	107.15(8)	103.96(8)	**1.6132(15)**	2.550(2)
O14	111.16(9)	110.79(8)	107.21(8)	**1.5456(14)**

Li1–O2 = 1.991(4)
Li1–O3 = 2.092(4)
Li1–O6 = 1.982(3)
Li1–O13 = 2.328(4)
Li1–O14 = 2.351(4)

Li2–O2 = 1.904(4)
Li2–O5 = 1.974(4)
Li2–O5 = 1.954(4)
Li2–O14 = 1.999(4)

Li3–O1 = 2.288(5)
Li3–O7 = 1.886(7)
Li3–O8 = 1.966(6)
Li3–O12 = 1.951(6)

Li4–O1 = 1.984(5)
Li4–O4 = 1.970(5)
Li4–O7 = 1.956(4)
Li4–O8 = 2.333(4)
Li4–O12 = 2.229(4)

Bold numbers are indicates they correspond to the Oi-Oi distances in the polyhedra.

$Ca_9MnLi(PO_4)_7$ [37] exhibits LiO_3 polyhedra and $LiMn(PO_4)((OD)_{0.442}(OH)_{0.558})$ [38] exhibits LiO_5 polyhedra. For the first time, a lithium manganese(II) phosphate exhibits two different kind of coordination polyhedra, LiO_4 and LiO_5, in the same framework. Moreover, among the manganese phosphates, to our knowledge, a five-fold coordination of lithium has only been observed in the manganese(III) phosphate $LiMn(PO_4)((OD)_{0.442}(OH)_{0.558})$ [38] up to now.

4. Conclusion

A new lithium manganese diphosphate, $Li_2MnP_2O_7$, has been synthesized. It exhibits a very original tunnel structure, characterized by the presence of Mn_2O_9 units, rarely observed for other manganese oxides. The arrangement of the lithium cations in the form of $[Li_2O_5]_\infty$ and $[Li_2O_6]_\infty$ layers is also quite original. It suggested us the possibility of cationic conductivity, eventually induced by Li deficiency. Unfortunately, the measurements performed on a sample of $Li_2MnP_2O_7$ did not revealed any ionic conductivity property. However, the above reported results illustrate the great structural diversity of the $A_2MP_2O_7$ family of compounds and suggest that other phases, with original topologies, could be isolated in the Li–Mn–P–O system.

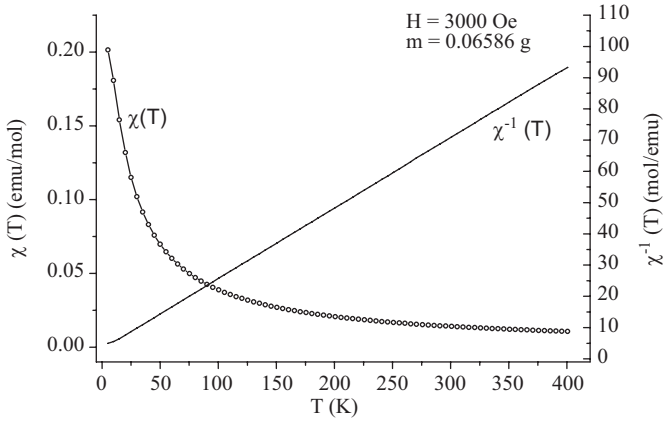

Fig. 4. Magnetic susceptibility χ versus temperature and the corresponding χ^{-1} versus T for $Li_2MnP_2O_7$.

Acknowledgment

Authors are grateful to Pr. V. Caignaert, Dr. V. Pralong and Dr. A. Pautrat for their help and fruitful discussions.

Appendix A. Supplementary materials

Supplementary data associated with this article can be found in the online version at doi:10.1016/j.jssc.2008.07.039

References

[1] A.K. Padhi, K.S. Nanjundaswamy, J.B. Goodenough, J. Electrochem. Soc. 144 (4) (1997) 1188–1194.
[2] A.S. Andersson, B. Kalska, L. Haggström, J.O. Thomas, Solid State Ionics 130 (2000) 41–52.
[3] S. Okada, S. Sawa, M. Egashira, J. Yamaki, M. Tabuchi, H. Kageyama, T. Konishi, A. Yoshino, J. Power Sources 97 (98) (2001) 430–432.
[4] M. Alvarez-Vega, O. Garcia-Moreno, F. Garcia-Alvardo, J. Garcia-Jaca, J.M. Gallardo-Amores, M.L. Sanjuan, U. Amador, Chem. Mater. 13 (2001) 1570–1576.
[5] J.M. Osorio-Guillen, B. Holm, R. Ahuja, B. Johansson, Solid State Ionics 167 (2004) 221–227.
[6] S. Geller, J.L. Durand, Acta Crystallogr. 13 (1960) 325–331.
[7] E.V. Murashova, N.N. Chudinova, Kristallografiya 46 (6) (2001) 1024–1029.
[8] L.S. Ivashkevich, K.A. Selevich, A.I. Lesnikovich, A.F. Selevich, A.S. Lyakhov, Z. Kristallogr. 221 (2) (2006) 115–121.
[9] M.T. Averbuch-Pouchot, Acta Crystallogr. C 45 (1989) 1856–1858.
[10] M.A.G. Aranda, J.P. Attfield, S. Bruque, Angew. Chem. (German Edit.) 104 (8) (1992) 1056–1058.
[11] M.T. Averbuch-Pouchot, A. Durif, J. Appl. Crystallogr. 5 (1972) 307.
[12] V. Petricek, M. Dusek, L. Palatinus, Jana2006. Structure Determination Software Programs, Institute of Physics, Praha, Czech Republic, 2006.
[13] A.J.M. Duisenberg, L.M.J. Kroon-Batenburg, A.M.M. Schreurs, J. Appl. Crystallogr. 36 (2003) 220–229.
[14] N.E. Brese, M.O' Keeffe, Acta Crystallogr. B 47 (1991) 192–197.
[15] R. Faggiani, C. Calvo, Can. J. Chem. 54 (1976) 3319–3324.
[16] V.K. Trunov, Yu.V. Oboznenko, S.P. Sirotinkin, N.B. Tskhelashvili, Izv. Akad. Nauk Neorg. Mater. 27 (1991) 1993–1994.
[17] V.K. Trunov, Yu.V. Oboznenko, S.P. Sirotinkin, N.B. Tskhelashvili, Izv. Akad. Nauk Neorg. Mater. 27 (1991) 2370–2374.
[18] A. El Maadi, A. Boukhari, E.M. Holt, S. Flandrois, C.R. Acad. Sci. II 318 (1994) 765–770.
[19] M. Sandstroem, A. Fischer, D. Bostroem, Acta Crystallogr. E 59 (2003) i139–i141.

[20] F. Erragh, A. Boukhari, B. Elouadi, E.M. Holt, J. Cryst. Spectrosc. 21 (21) (1991) 321–326.
[21] Y. Laligant, Eur. J. Solid State Inor. Chem. 29 (1992) 239–247.
[22] M.R. Spirlet, J. Rebizant, M. Liegeois-Duyckaerts, Acta Crystallogr. C 49 (1993) 209–211.
[23] F. Erragh, A. Boukhari, A. Sadel, E.M. Holt, Acta Crystallogr. C 54 (1998) 1373–1376.
[24] I. Belharouak, C. Parent, P. Gravereau, J.P. Chaminade, G. Le Flem, B. Moine, J. Solid State Chem. 149 (2000) 284–291.
[25] K.M.S. Etheredge, S.J. Hwu, Inorg. Chem. 34 (1995) 1495–1499.
[26] F. Erragh, A. Boukhari, F. Abraham, B. Elouadi, J. Solid State Chem. 120 (1995) 23–31.
[27] Y. Laligant, Eur. J. Solid State Inor. Chem. 29 (1992) 83–94.
[28] I. Belharouak, P. Gravereau, C. Parent, J.P. Chaminade, E. Lebraud, G. Le Flem, J. Solid State Chem. 152 (2000) 466–473.
[29] Yu.F. Shepelev, M.A. Petrova, A.S. Novikova, A.E. Lapshin, Glass Phys. Chem. 28 (5) (2002) 317–321.
[30] A.El. Maadi, J. Bennazha, J.M. Reau, A. Boukhari, E.M. Holt, Mater. Res. Bull. 38 (2003) 865–874.
[31] Q. Huang, S.J. Hwu, Inorg. Chem. 37 (1998) 5869–5874.
[32] A. ElMaadi, A. Boukhari, E.M. Holt, J. Chem. Crystallogr. 25 (9) (1995) 531–536.
[33] N. Stock, Z. Naturforsch. B57 (2002) 187–192.
[34] A. Riou, Y. Cudennec, Y. Gerault, Acta Crystallogr. C57 (1987) 821–823.
[35] P. Lightfoot, A.K. Cheetham, J. Chem. Soc. Dalton Inorg. Chem. 89 (1989) 1765–1769.
[36] W. Massa, O.V. Yakubovich, O.V. Dimitrova, Solid State Sci. 7 (2005) 950–956.
[37] A.A. Belik, V.B. Gutan, L.N. Ivanov, B.I. Lazoryak, Zh. Neorg. Khim. 46 (6) (2001) 885–892.
[38] M.A.G. Aranda, S. Bruque, J.P. Attfield, F. Palacio, R.B. von Dreele, J. Solid State Chem. 132 (1997) 202–212.